Available online at www.sciencedirect.com

SciVerse ScienceDirect

Procedia Engineering 00 (2016) 000–000

Procedia Engineering

www.elsevier.com/locate/procedia

25th International Meshing Roundtable

On Tetrahedralisations of Reduced Chazelle Polyhedra with Interior Steiner Points

Hang Si, Nadja Goerigk

Weierstrass Institute for Applied Analysis and Stochastics (WIAS)
Mohrenstrasse 39, 10117 Berlin, Germany

Abstract

The non-convex polyhedron constructed by Chazelle, known as the *Chazelle polyhedron* [4], establishes a quadratic lower bound on the minimum number of convex pieces for the 3d polyhedron partitioning problem. In this paper, we study the problem of tetrahedralising the Chazelle polyhedron without modifying its exterior boundary. It is motivated by a crucial step in tetrahedral mesh generation in which a set of arbitrary constraints (edges or faces) need to be entirely preserved. The goal of this study is to gain more knowledge about the family of 3d indecomposable polyhedra which needs additional points, so-called *Steiner points*, to be tetrahedralised. The requirement of only using interior Steiner points for the Chazelle polyhedron is extremely challenging. We first "cut off" the volume of the Chazelle polyhedron by removing the regions that are tetrahedralisable. This leads to a 3d non-convex polyhedron whose vertices are all in the two slightly shifted saddle surfaces which are used to construct the Chazelle polyhedron. We call it the *reduced Chazelle polyhedron*. It is an indecomposable polyhedron. We then give a set of $(N+1)^2$ interior Steiner points that ensures the existence of a tetrahedralisation of the reduced Chazelle polyhedron with $4(N+1)$ vertices. The proof is done by transforming a 3d tetrahedralisation problem into a 2d edge flip problem. In particular, we design an edge splitting and flipping algorithm and prove that it gives to a tetrahedralisation of the reduced Chazelle polyhedron.

Peer-review under responsibility of the organizing committee of IMR 25.

Keywords: Non-convex polyhedron; Indecomposable polyhedron; tetrahedralisation; Chazelle polyhedron; Schönhardt polyhedron; Steiner points; edge flip

1. Introduction

A theoretical difficulty in many geometric problems is the existence of 3d *indecomposable polyhedra*, which are non-convex 3d polyhedra whose interior cannot be decomposed into a set of non-overlapping tetrahedra whose vertices are all of the given polyhedra, such as the well-known Schönhardt polyhedron [17] and some generalisation of it [1, 10,15]. Meanwhile, it is NP-complete to determine whether a given 3d non-convex polyhedron can be tetrahedralised

* Hang Si. Tel.: +49-30-20372-446 ; fax: +49-30-20372-303.
E-mail address: Hang.Si@wias-berlin.de

Peer-review under responsibility of the organizing committee of IMR 25.

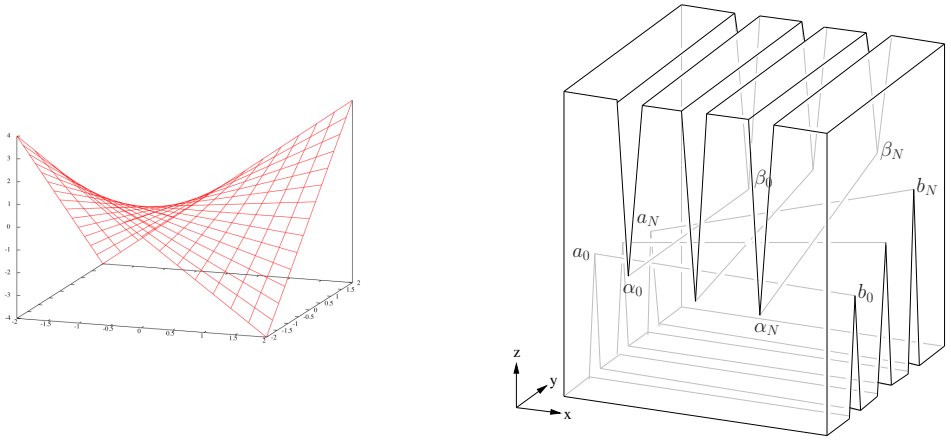

Fig. 1. Left: A saddle surface (a hyperbolic paraboloid). Right: The Chazelle polyhedron [4] with three notches, i.e., $N = 2$, on the top and the bottom faces, respectively.

in this way [16]. Although it is known that any indecomposable polyhedra can be tetrahedralised by inserting a certain number of additional points, so-called *Steiner points*, it remains unknown, for an arbitrary 3d polyhedron, how many Steiner points are required and where these Steiner points should be located.

The polyhedron constructed by Chazelle, known as the *Chazelle polyhedron* [4], see Figure 1, is an important example in many partitioning problems. The core of the Chazelle polyhedron consists of two sets of line segments that lie on two slightly shifted doubly-ruled hyperbolic surfaces (saddle surfaces). The space between these two saddle surfaces forms an 3d indecomposable polyhedron. The Chazelle polyhedron was initially used to prove a quadratic lower bound on the complexity of convex decomposition of 3d polyhedron [4]. It becomes a useful example to construct lower bounds in many other problems, such as the binary space partition problem [14], the bounding volume hierarchy for collision detection problem [7], the decomposablility of fat-polyhedra [6], and the optimal tetrahedralisation (in terms of size and shape of mesh elements) in finite element mesh generation [3].

If Steiner points are allowed to be placed on the boundary of a 3d polyhedron, then there are many solutions. For example, the algorithm of Chazelle and Palios [4,5] decomposes any 3d polyhedron of genus zero with n vertices and r reflex edges (a measure of non-convexity) into $O(n + r^2)$ tetrahedra in $O((n + r^2) \log r)$ time. There are efficient algorithms to generate a constrained Delaunay tetrahedralisation [19] of any 3d polyhedra [12,18,20–22].

In this paper, we study the problem of tetrahedralising the Chazelle polyhedron without modifying its exterior boundary, which means, Steiner points are only placed in the interior of it. The restriction of the locations of Steiner points in the interior makes this problem harder than the original convex decomposition problem that has been studied before [5]. This requirement stems from a crucial step in finite element mesh generation – the *boundary recovery problem* [8,9,20,26], in which a given set of *constraints* (edges or faces) must be entirely preserved in the final meshes. Such constraints are required in various purposes, such as to assign boundary conditions, to access the geometric information, to match another partition sharing at the common interface, to generate anisotropic meshes (whose elements are aligned along certain directions), etc.

A classical method to handle this problem is to start with an initial tetrahedralisation, like the Delaunay tetrahedralisation, of the vertices of the polyhedron, and then to recover the missing constraints by locally modifying the mesh through a set of *local mesh transformation operations*, such as edge and face flips, vertex insertion and deletion. All these operations take an input of a *cavity* which is a 3d polyhedron formed by the union of a set of existing tetrahedra and return a set of new tetrahedra that fills the interior of the cavity without modifying its outer boundary. The shape of the cavity is a 3d polyhedron which is not necessarily convex. In many cases, the presented cavity has a simple shape so that a missing constraint can be easily recovered by only performing flips. However, if a cavity is an indecomposable polyhedron, interior Steiner points are needed in order to complete the tetrahedralisation process.

Since it is difficult to detect whether a cavity is tetrahedralisable in advance, many heuristics methods are developed. Most of the approaches first try using flips as much as possible, then try adding Steiner points [9], or interchange these two operations [8,20,26]. In practice, all these approaches worked very well. However, it is not surprising that they

may fail unexpectedly on some special inputs. As an example, we tested two codes (INRIA's `Tetmesh-GHS3D` [24] and `TetGen` [20]) on a Chazelle polyhedron with a rather small number of input vertices, both of these codes run much slower compared with other inputs, and produced very different numbers of interior Steiner points. Moreover, when we made the volume of the Chazelle polyhedron slightly smaller, both codes failed to produce a valid output [1].

A theoretical difficulty in these algorithms is due to the fact that there is a lack of knowledge about the geometry and combinatorial structures of the whole family of 3d indecomposable polyhedra. There are only few works [2,6,7, 11,25] on these topics. In [10], we proved the optimal number of interior Steiner points for some 3d indecomposable polyhedra whose geometric structures are understood, such as the Schönhardt polyhedron, Bagemihl polyhedron, and a more general class of them. This result provides useful suggestion to design correct and efficient algorithms to tetrahedralise such polyhedra. However, the geometry and combinatorial structures of 3d indecomposable polyhedra are largely unknown. Therefore, it is meaningful to consider these answers for some specific types of indecomposable polyhedra, such as the Chazelle polyhedra. Our goal is to gain knowledge of 3d indecomposable polyhedra by understanding how to decompose Chazelle polyhedra.

The remainder of this paper is organised as follows: In Section 2 we briefly review the construction of the Chazelle polyhedron, and discuss its basic properties. In Section 3 we perform a polyhedral reduction of the Chazelle polyhedron by removing polyhedra which are tetrahedralisable. This leads to a 3d indecomposable polyhedron, which will be defined as the reduced Chazelle polyhedron $\Phi_{N,\varepsilon}$ with the two parameters N and ε. We then study how to tetrahedralise the reduced Chazelle polyhedron by placing only interior Steiner points in Section 4. We first place a set of N^2 interior Steiner points in the interior of a reduced Chazelle polyhedron $\Phi_{N,\varepsilon}$, and then we prove that there exists a tetrahedralisation of $\Phi_{N,\varepsilon}$ with this set of Steiner points. There is a correspondence between a sequence of edge flips and a tetrahedralisation of a 3d polyhedron. This allows us to transform our 3d tetrahedralisation problem into a 2d triangulation transformation problem. A difficulty is due to the non-convexity of the reduced Chazelle polyhedron. We show that every edge flip generated by our transformation algorithm corresponds to a valid tetrahedron in $\Phi_{N,\varepsilon}$. Finally, we discuss some open issues in Section 5.

2. The Chazelle Polyhedron

The essential geometry of a Chazelle polyhedron is a saddle surface, which is a hyperbolic paraboloid, specified by the equation $z = x^2 - y^2$ or $z = xy$, see Figure 1 left. It is a doubly ruled surface which means that it can be made by two different sets of lines.

The Chazelle polyhedron is constructed by cutting notches from the two opposite faces of a cube, see Figure 1 right. Place the bottom face of the cube in the xy-plane and aligning its edges with the x- and y-axis. Call the notches on top and bottom of the cube *top notches* and *bottom notches*, respectively. Let all the bottom notches be parallel to the y-axis and lie on the saddle surface $z = xy$, and let all the top notches be parallel to the x-axis and lie on the saddle surface $z = xy + \varepsilon$, for a small positive constant $\varepsilon > 0$. In general, there may be an arbitrary number of notches. This leads to a family of such polyhedra which are parametrised by the number of notches N and the thickness ε.

Assume there are $N + 1$ notches on each face of the cube, where $N \geq 1$. Label the vertices of the top and bottom notches as: a_i, b_i, α_i, and β_i, where $i = 0, \ldots, N$, respectively (see Figure 1 Right). A choice of the coordinates of these vertices given by Chazelle is:

$$
\begin{aligned}
a_i &:= (-1, i, -i),\\
b_i &:= (N + 1, i, i(N + 1)),\\
\alpha_i &:= (i, -1, -i + \varepsilon),\\
\beta_i &:= (i, N + 1, i(N + 1) + \varepsilon),
\end{aligned}
$$

for integers $0 \leq i \leq N$. Therefore, the length of the top and bottom faces of the cube is $N + 2$. The lower face of the cube lies below the plane $z = -N$, and the top face of the cube lies above the plane $z = N(N + 1) + \varepsilon$.

Let $\Pi_{N,\varepsilon}$ be a Chazelle polyhedron with $N + 1$ notches and a thickness ε. Let Σ be the region between the two hyperbolic paraboloids in $\Pi_{N,\varepsilon}$. If ε is sufficiently small, Σ has volume $\Theta(\varepsilon N^2)$, and every convex polyhedron that lies

[1] We plan to make our testing examples available in `TetGen`'s website `http://www.tetgen.org` in the future

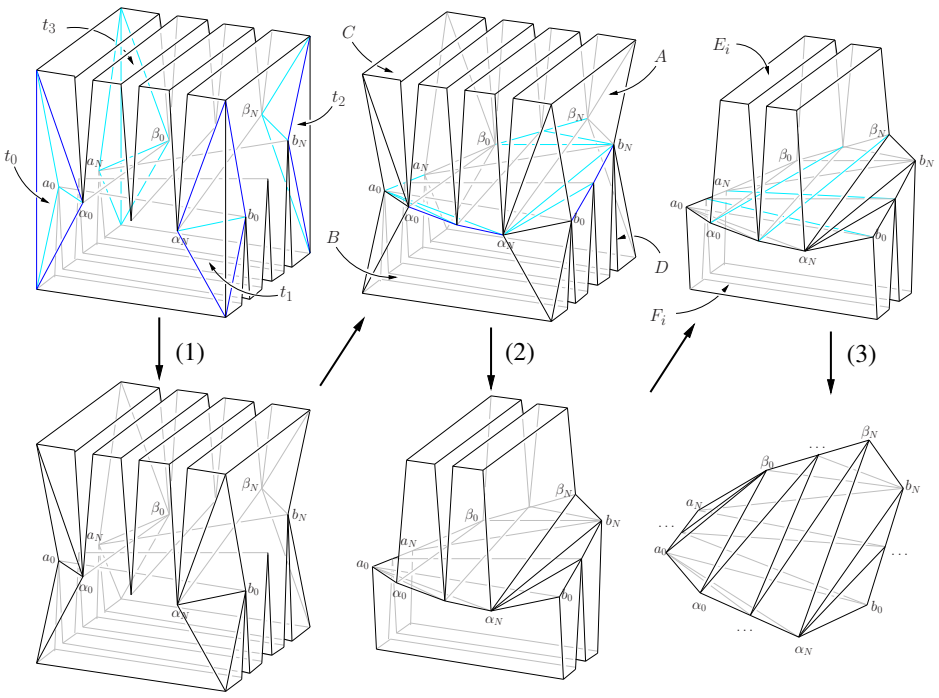

Fig. 2. The volume reduction process. The three steps of the reduction are shown by the arrows. It starts from the Chazelle polyhedron (top-left) and ends at the reduced Chazelle polyhedron (bottom-right). At each step, a set of interior edges (shown in blue) is first inserted, and then a number of tetrahedra $t_1, \ldots, t_4$, and polyhedra: $A, B, C, D, E_1, \ldots, E_N$, and $F_1, \ldots, F_N$ are removed.

in Σ necessarily has volume $o(\varepsilon)$ or smaller. These two facts are enough to show that Σ needs at least $\Omega(N^2)$ convex polyhedra to be decomposed. This also implies that it needs many Steiner points to be tetrahedralised.

Indeed the real problematic part in $\Pi_{N,\varepsilon}$ is the region Σ, which is the space formed between the two saddle surfaces. This region can be made arbitrarily small by letting $\varepsilon \to 0$, which can cause the failure of many existing tetrahedralisation algorithms. In the next section, we will study the geometric structure of Σ.

3. Reduced Chazelle Polyhedra

3.1. A Volume Reduction of the Chazelle Polyhedron

Let $\Pi_{N,\varepsilon}$ be the Chazelle polyhedron with $N+1$ notches and a thickness ε. In this section, we will reduce the volume of $\Pi_{N,\varepsilon}$ by removing the regions that are tetrahedralisable until it is not possible anymore. Our reduction is done in three steps. In each step, we will insert some interior edges into $\Pi_{N,\varepsilon}$. This allows us to remove some regions which are tetrahedralisable. These steps are described below (see also Figure 2):

Step (1). This step first inserts the four interior edges of $\Pi_{N,\varepsilon}$:

$$a_0\alpha_0, b_0\alpha_N, a_N\beta_0, \text{ and } b_N\beta_N.$$

It then removes the four (corner) tetrahedra: $t_0, \ldots, t_3$ from $\Pi_{N,\varepsilon}$.

Step (2). This step first inserts the following interior edges of $\Pi_{N,\varepsilon}$:

$$\begin{aligned}&\{\alpha_N b_i, a_0\alpha_i \mid i = 1, \ldots, N\},\\ \cup\ &\{\beta_0 a_i, b_N\beta_i \mid i = 0, \ldots, N-1\},\\ \cup\ &\{a_i a_{i+1}, b_i b_{i+1}, \alpha_i\alpha_{i+1}, \beta_i\beta_{i+1} \mid i = 0, \ldots, N-1\}.\end{aligned}$$

It then removes the four corner polyhedra: A, B, C, and D from $\Pi_{N,\varepsilon}$.

Step (3). This step first inserts the following interior edges of $\Pi_{N,\varepsilon}$:

$$\{\alpha_i\beta_j \,|\, i = 0,\ldots,N-1 \text{ and } j = 1,\ldots,N\}$$
$$\cup\, \{a_ib_j \,|\, i = 1,\ldots,N \text{ and } j = 0,\ldots,N-1\}$$

Then it removes the $2N$ polyhedra: $E_1,\ldots,E_N$ and $F_1,\ldots,F_N$ of $\Pi_{N,\varepsilon}$.

At the end of this reduction process, we obtain a polyhedron $\Phi_{N,\varepsilon} \subset \Pi_{N,\varepsilon}$, where

$$\Phi_{N,\varepsilon} := \Pi_{N,\varepsilon} - (t_0 + \ldots, t_3) - (A + B + C + D) - (E_1 + \ldots + E_N) - (F_1 + \ldots + F_N).$$

The vertices of $\Phi_{N,\varepsilon}$ are endpoints of the two sets of lines on the two saddle surfaces $z = xy$ and $z = xy + \varepsilon$. We will call $\Phi_{N,\varepsilon}$ the *reduced Chazelle polyhedron*.

It can be shown that all the regions that have been removed from the original Chazelle polyhedron, i.e., $t_0,\ldots,t_3$, A, B, C, D, $E_1,\ldots,E_N$ and $F_1,\ldots,F_N$ are all tetrahedralisable with a linear number of tetrahedra (see Appendix). Therefore the reason that causes the Chazelle polyhedron to be indecomposable is due to the reduced Chazelle polyhedron.

3.2. A Direct Definition of the Reduced Chazelle Polyhedron

Alternatively, we can define the *reduced Chazelle polyhedron* $\Phi_{N,\varepsilon}$ as follows (refer to Figure 3 left):

The set of vertices of $\Phi_{N,\varepsilon}$ are

$$\{a_i, b_i, \alpha_i, \beta_i \,|\, i = 0,\ldots,N\},$$

where

$$a_i := (-1, i, -i), \text{ and } b_i := (N+1, i, i(N+1)),$$

are endpoints of the line segments on the saddle surface $z = xy$, and

$$\alpha_i := (i, -1, -i + \varepsilon), \text{ and } \beta_i := (i, N+1, i(N+1) + \varepsilon),$$

are endpoints of the line segments on $z = xy + \varepsilon$.

This is a non-convex polyhedron. In the following, we explicitly list the set of faces and edges of this polyhedron, refer to Figure 3 left.

The set of triangular faces of $\Phi_{N,\varepsilon}$ are:

(1) $\{\alpha_i\beta_{i+1}\beta_i, \alpha_i\beta_{i+1}\alpha_{i+1} \,|\, i = 0,\ldots,N-1\}$;
(2) $\{\alpha_Nb_ib_{i+1}, \beta_0a_ia_{i+1} \,|\, i = 0,\ldots,N-1\}$;
(3) $\{\alpha_Nb_N\beta_N, \beta_0a_0\alpha_0\}$;
(4) $\{a_{i+1}b_ia_i, a_{i+1}b_ib_{i+1} \,|\, i = 0,\ldots,N-1\}$;
(5) $\{a_0\alpha_i\alpha_{i+1}, b_N\beta_i\beta_{i+1} \,|\, i = 0,\ldots,N-1\}$.
(6) $\{a_0\alpha_Nb_0, b_N\beta_0\alpha_N\}$;

The triangles in sets (1), (2) and (3) are called *top triangles* of $\Phi_{N,\varepsilon}$, and the triangles in sets (4), (5), and (6) are called *bottom triangles* of $\Phi_{N,\varepsilon}$, as they are viewed from the top of the xy-plane, see Figure 3. In particular, the top triangles and bottom triangles form two triangulations of a convex polygon, they are called the *top triangulation* $\mathcal{T}_t$ and the *bottom triangulation* $\mathcal{T}_b$ of $\Phi_{N,\varepsilon}$, respectively. The parameter ε is called the *thickness* of $\Phi_{N,\varepsilon}$.

The set of edges of $\Phi_{N,\varepsilon}$ can be divided into three groups, which are locally non-convex edge (relax edges), locally convex edges, and planar edges. They are listed below.

There are two set of locally non-convex edges (reflex edges) which belong to the two saddle surfaces, respectably. They are:

(7) $\{\alpha_i\beta_i \,|\, i = 0,\ldots,N\}$
(8) $\{a_ib_i \,|\, i = 0,\ldots,N\}$

where (7) and (8) are edges in top and bottom triangulations, respectively.

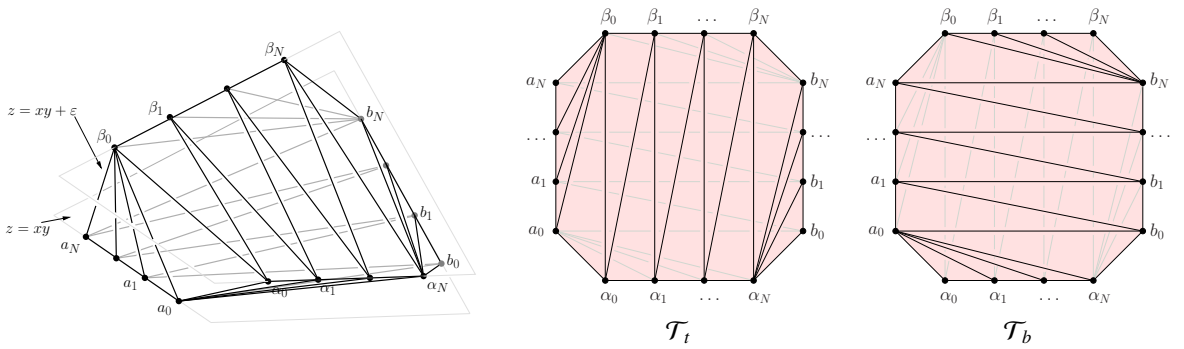

Fig. 3. Left: A reduced Chazelle polyhedron $\Phi_{3,\varepsilon}$. Right: The top triangulation $\mathcal{T}_t$ includes the set of top faces as viewed from the point $(0, 0, +\infty)$ toward the $-z$ direction. The bottom triangulation $\mathcal{T}_b$ includes the set of bottom faces viewed from the point $(0, 0, -\infty)$ toward the $+z$ direction.

The locally convex edges are described in the following seven sets, respectively. They are:

(9) $\{\alpha_i\beta_{i+1} \,|\, i = 0, \ldots, N-1\}$
(10) $\{a_{i+1}b_i \,|\, i = 0, \ldots, N-1\}$
(11) $\{\alpha_i\alpha_{i+1} \,|\, i = 0, \ldots, N-1\}$
(12) $\{\beta_i\beta_{i+1} \,|\, i = 0, \ldots, N-1\}$
(13) $\{a_ia_{i+1} \,|\, i = 0, \ldots, N-1\}$
(14) $\{b_ib_{i+1} \,|\, i = 0, \ldots, N-1\}$
(15) $\{\alpha_0a_0, \alpha_Nb_0, b_N\beta_N, \beta_0\alpha_N\}$

where (9) and (10) are edges in top and bottom triangulations, respectively. And (11), (12), (13), (14), and (15) are the common boundary edges of the top and bottom triangulations.

There are four sets of planar edges, which are:

(16) $\{\alpha_Nb_{i+1} \,|\, i = 0, \ldots, N-1\}$
(17) $\{\beta_0a_{i+1} \,|\, i = 0, \ldots, N-1\}$
(18) $\{a_0\alpha_{i+1} \,|\, i = 0, \ldots, N-1\}$
(19) $\{b_N\beta_{i+1} \,|\, i = 0, \ldots, N-1\}$

where (16) and (17) are edges in top triangulations, and (18) and (19) are edges in bottom triangulations, respectively.

In summary, the reduced Chazelle polyhedron $\Phi_{N,\varepsilon}$ has $4(N+1) = 4N+4$ vertices, $2(N+1)+6N+4+4N = 12N+6$ edges, and $8N + 4$ faces. It is a simple polyhedron verified by the Euler formula. Note that only $2N + 2$ edges are locally non-convex (reflex edge), which are the sets (7) and (8). Moreover, if the parameter ε is small enough, no other edge from the vertices of the polyhedron can lie entirely inside the polyhedron. This implies that $\Phi_{N,\varepsilon}$ is an indecomposable polyhedron.

4. Tetrahedralisations of Reduced Chazelle Polyhedra

In this section, we consider our main question: to tetrahedralise a reduced Chazelle polyhedron $\Phi_{N,\varepsilon}$ without modifying its exterior boundary. For this purpose, Steiner points can be only added in the interior of $\Phi_{N,\varepsilon}$. We will propose a set of interior Steiner points in $\Phi_{N,\varepsilon}$ and show there exists a tetrahedralisation of $\Phi_{N,\varepsilon}$ with this set of Steiner points. Before we do that, we will review a nice relation between a sequence of edge flips and a tetrahedralisation of a 3d polyhedron. This allows us to transform our tetrahedralisation problem to a 2d triangulation transformation problem.

4.1. Edge Flips and Tetrahedralisations

If we ignore the z-coordinates of the vertices of $\Phi_{N,\varepsilon}$, the top and bottom faces of $\Phi_{N,\varepsilon}$ give two different triangulations of a two-dimensional convex polygon Q whose vertices are vertices of $\Phi_{N,\varepsilon}$ projecting onto the xy-plane, see

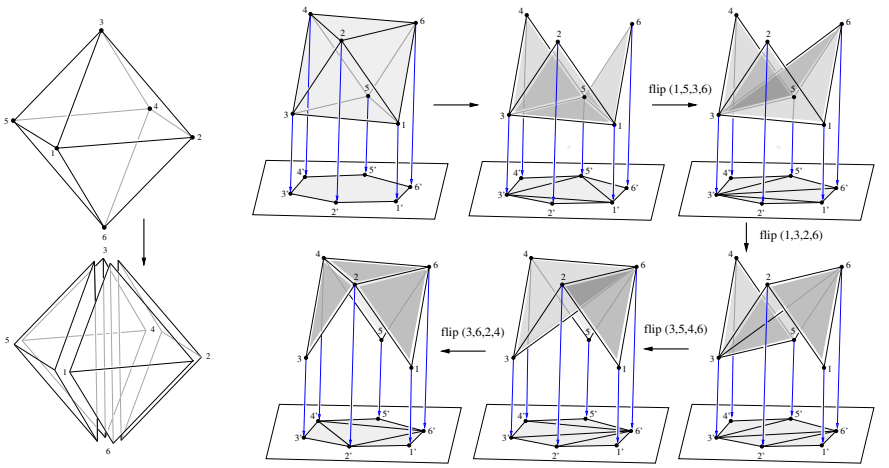

Fig. 4. Left: A tetrahedralisation of an octahedron with four tetrahedra. Right: A sequence of edge flips which corresponds to the tetrahedralisation on the left.

Figure 3. It is well known that there exists a sequence of edge flips that will transform one triangulation to another one of Q [13].

Sleator et al [23] showed the correspondence between a sequence of edge flips and a tetrahedralisation of a 3d convex polyhedron. The basic idea is to view every edge flip as removing a tetrahedron from the polyhedron. By fixing a position of a 3d convex polyhedron P, the orthogonal projection of P (i.e., ignoring the z-coordinates of points in P) is a convex polygon Q in the xy-plane. At this moment, one only "sees" the outer boundary faces of P which is a 2d triangulation $\mathcal{T}_1$ of Q. Now an edge flip in $\mathcal{T}_1$ corresponds the removal of a tetrahedron from P such that the two lower faces of this tetrahedron are replaced by the two upper faces of it. After a sequence of such edge flips, the hidden boundary faces of P, which is another triangulation $\mathcal{T}_2$ of Q, appears. As a consequence, the collection of removed tetrahedra and their faces gives a tetrahedralisation of P. Moreover, the length of the flip sequence is equal to the total number of tetrahedra in this tetrahedralisation. The example of Sleator et al [23] is reproduced (correctly) in Figure 4.

However, not every tetrahedralisation of a 3d polyhedron is associated to a sequence of flips. This is even true for convex polyhedra, as shown in Sleator et al [23]. A reduced Chazelle polyhedron $\Phi_{N,\varepsilon}$ is non-convex. The main problem caused by the non-convexity is that a flippable edge in the plane may not correspond to a valid tetrahedron in the interior of a non-convex polyhedron. Indeed, it is possible that none of the flippable edges in the top and bottom triangulation of $\Phi_{N,\varepsilon}$ will create a valid tetrahedron in the interior of $\Phi_{N,\varepsilon}$. This problem can only be resolved if there are Steiner points in $\Phi_{N,\varepsilon}$.

4.2. A Placement of Interior Steiner Points

Recall that the volume of a Chazelle polyhedron $\Phi_{N,\varepsilon}$ is sandwiched by two saddle surfaces with a thickness ε. We will place a set of $(N+1)^2$ interior Steiner points,

$$\mathcal{S} := \{s_{i,j} \mid i, j = 0, \ldots, N\},$$

where

$$s_{i,j} := (i, j, ij + \omega), \text{ and } 0 < \omega < \varepsilon,$$

into the interior of $\Phi_{N,\varepsilon}$. These Steiner points are directly at the intersections of the two set of lines in the xy-plane and all lie on the saddle surface $z = xy + \omega$, where $0 < \omega < \varepsilon$, see Figure 5. We will show that there exists a tetrahedralization of a reduced Chazelle polyhedron $\Phi_{N,\varepsilon}$ with this set of Steiner points.

Due to the correspondence of edges flips and tetrahedralisations, we will tackle our tetrahedralisation problem by using two-dimensional triangulations. In particular, we will first show a transformation between the two triangulations

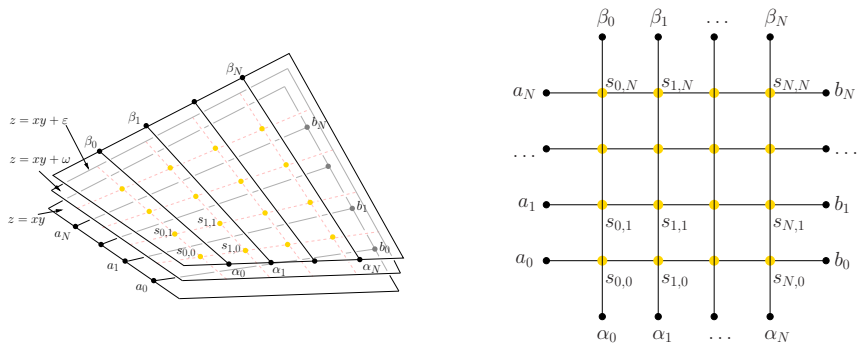

Fig. 5. The interior Steiner points, $\{s_{i,j} \mid i, j = 0, \ldots, N\}$, are placed directly at the intersections of the two set of lines in the xy-plane and all lie on the saddle surface $z = xy + \omega$, where $0 < \omega < \varepsilon$.

$\mathcal{T}_t$ and $\mathcal{T}_b$ (shown in Figure 3), which includes the set $\mathcal{S}$ of Steiner points. And then show this transformation indeed corresponds to a tetrahedralisation of $\Phi_{N,\varepsilon}$.

4.3. The Transformation Algorithm

To simplify the transformation algorithm as well as our proof, it is more convenient to work on a modified polyhedron, denoted $\Phi^s_{N,\varepsilon}$. It is only different to $\Phi_{N,\varepsilon}$ at the four corners. The modifications are summarised in the following.

- Introduce four new Steiner points on the saddle surface $z = xy + \omega$, they are located on the corners of $\Phi_{N,\varepsilon}$, i.e., let

$$\mathcal{S}^s := \mathcal{S} \cup \{s_{-1,-1}, s_{-1,N+1}, s_{N+1,-1}, s_{N+1,N+1}\},$$

  where

$$\begin{aligned} s_{-1,-1} &:= (-1, -1, 1 + \omega), \\ s_{-1,N+1} &:= (-1, N + 1, -(N + 1) + \omega), \\ s_{N+1,-1} &:= (N + 1, -1, -(N + 1) + \omega), \\ s_{N+1,N+1} &:= (N + 1, N + 1, (N + 1)^2 + \omega). \end{aligned}$$

- Relabelling the vertices of $\mathcal{T}_t$ and $\mathcal{T}_b$ as following:

$$\begin{aligned} a_0 &\to s_{-1,0}, \quad \ldots, a_N \to s_{-1,N} \\ b_0 &\to s_{N+1,0}, \ldots, b_N \to s_{N+1,N} \\ \alpha_0 &\to s_{0,-1}, \quad \ldots, \alpha_N \to s_{N,-1} \\ \beta_0 &\to s_{0,N+1}, \ldots, \beta_N \to s_{N,N+1} \end{aligned}$$

- Modify $\mathcal{T}_t$ and $\mathcal{T}_b$ to include the new Steiner points, i.e., let

$$\begin{aligned} \mathcal{T}^s_t := \mathcal{T}_t &\setminus \{s_{-1,0}s_{0,-1}s_{0,N+1}, s_{N,-1}s_{N,N+1}s_{N+1,N}\} \\ &\cup \{s_{-1,-1}s_{0,N+1}s_{-1,0}, s_{-1,-1}s_{0,N+1}s_{0,-1}, s_{-1,N}s_{0,N+1}s_{-1,N+1}\} \\ &\cup \{s_{N,-1}s_{N+1,N+1}s_{N,N+1}, s_{N,-1}s_{N+1,N+1}s_{N+1,N}, s_{N,-1}s_{N+1,-1}s_{N+1,0}\}, \end{aligned}$$

  and

$$\begin{aligned} \mathcal{T}^s_b := \mathcal{T}_b &\setminus \{s_{-1,0}s_{N+1,0}s_{N,-1}, s_{N+1,N}s_{-1,N}s_{-1,N+1}\} \\ &\cup \{s_{-1,0}s_{N+1,-1}s_{N,-1}, s_{-1,0}s_{N+1,-1}s_{N+1,0}, s_{-1,-1}s_{-1,0}s_{0,-1}\} \\ &\cup \{s_{N,-1}s_{N+1,N+1}s_{N,N+1}, s_{N,-1}s_{N+1,N+1}s_{N+1,N}, s_{N,-1}s_{N+1,-1}s_{N+1,0}\}. \end{aligned}$$

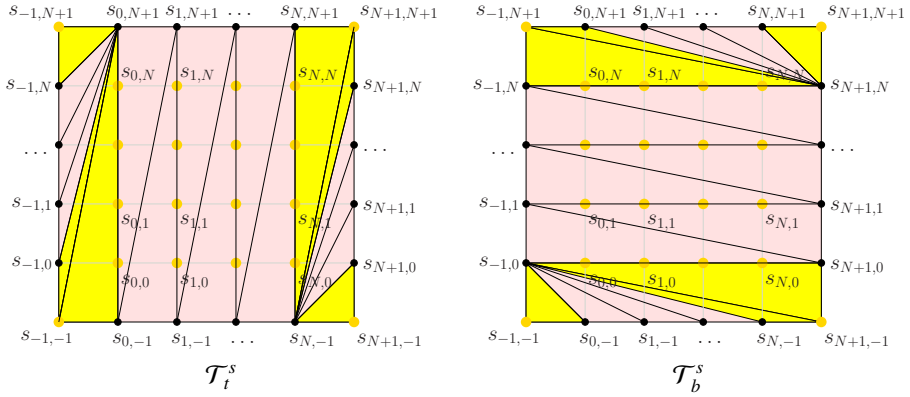

Fig. 6. The modified top and bottom triangulations of $\Phi^s_{N,\varepsilon}$. There are four new vertices: $s_{-1,-1}$, $s_{N+1,-1}$, $s_{-1,N+1}$, and $s_{N+1,N+1}$. The newly added triangles are shown in yellow.

Figure 6 illustrates an example after making these modifications on the example in Figure 3. The volume of the original reduced Chazelle polyhedron $\Phi_{N,\varepsilon}$ is completely included in the modified reduced Chazelle polyhedron $\Phi^s_{N,\varepsilon}$. Although the transformation algorithm described below will only apply to the modified reduced Chazelle polyhedron $\Phi^s_{N,\varepsilon}$, this technique also applies to tetrahedralise the reduced Chazelle polyhedron $\Phi_{N,\varepsilon}$.

From now on, we will focus on the tetrahedralisation of the modified reduced Chazelle polyhedron $\Phi^s_{N,\varepsilon}$ with the set $\mathcal{S}$ of interior Steiner points.

Our algorithm will use two basic local transformation operations: `split_edge` and `flip_edge`, which are defined below.

- The `split_edge`(a, b, p) operation takes an edge ab and a point p that lies in the interior of ab as inputs. It replaces the two triangles abc and bad sharing at the edge ab by four triangles apc, bpc, apd, and bpd.
- The `flip_edge`(a, b, c, d) operation takes two triangles abc and bad sharing at the edge ab, and replaces them by another two triangles cda, and cdb sharing at the edge cd.

INPUT: $\mathcal{T}_t^s$

```
1   // inserting Steiner points
2   for I = 0 to N do
3       for J = 0 to N do
4           split_edge(s_{I,J-1}, s_{I,N+1}, s_{I,J});
5       endfor
6   endfor
7   // flipping edges
8   for I = 0 to ⌊(N+2)/2⌋ do
9       // flipping upper edges
10      for J = 0 to N + 1 do
11          for K = I to N − I do
12              edge_flip(s_{J+1,N+1−I}, s_{J,K−1}, s_{J+1,N−I}, s_{J,K})
13          endfor
14      endfor
15      // flipping lower edges
16      for J = 0 to N + 1 do
17          for K = I + 1 to N − I do
18              edge_flip(s_{J,I−1}, s_{J+1,N+1−K}, s_{J,I}, s_{J+1,N−K})
19          endfor
20      endfor
21  endfor
22  return T_t^m;
```

INPUT: $\mathcal{T}_b^s$

```
1   // inserting Steiner points
2   for I = 0 to N do
3       for J = 0 to N do
4           split_edge(s_{I−1,J}, s_{N+1,J}, s_{I,J});
5       endfor
6   endfor
7   // flipping edges
8   for I = 0 to ⌊(N+2)/2⌋ do
9       // flipping left edges
10      for J = 0 to N + 1 do
11          for K = I to N − I do
12              edge_flip(s_{I−1,J}, s_{N+1−K,J−1}, s_{I,J}, s_{N−K,J−1})
13          endfor
14      endfor
15      // flipping right edges
16      for J = 0 to N + 1 do
17          for K = I + 1 to N − I do
18              edge_flip(s_{N+1−I,J−1}, s_{K−1,J}, s_{N−I,J−1}, s_{K,J})
19          endfor
20      endfor
21  endfor
22  return T_b^m;
```

Fig. 7. The transformation algorithm. It is divided into two parts, where one works in the top triangulation $\mathcal{T}_t^s$, and the other works in the bottom triangulation $\mathcal{T}_b^s$.

Our algorithm is given in Figure 7. This algorithm transforms the two triangulations, $\mathcal{T}_t^s$ and $\mathcal{T}_b^s$, simultaneously. It works in two steps. In the first step, it uses `split_edge` operations to insert the interior Steiner points into both $\mathcal{T}_t^s$ and $\mathcal{T}_b^s$. In the second step, it uses `edge_flip` operations to transform $\mathcal{T}_t^s$ and $\mathcal{T}_b^s$ into two *middle triangulations*, $\mathcal{T}_t^m$ and $\mathcal{T}_b^m$, respectively. An example of this algorithm is shown in Figures 8 and 9.

Note that the two resulting triangulations $\mathcal{T}_t^m$ and $\mathcal{T}_b^m$ are only different by $(N+1)^2$ diagonal flips. Hence this algorithm will successfully transform $\mathcal{T}_t^s$ to $\mathcal{T}_b^s$ or vice versa.

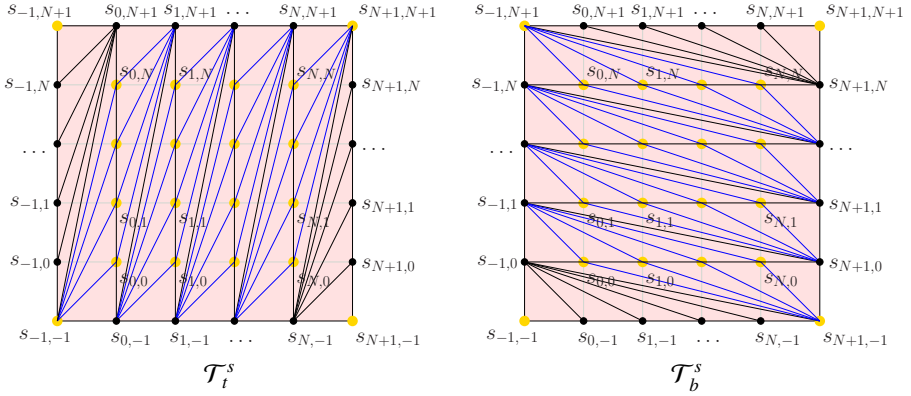

Fig. 8. An example result of the first step of the transformation algorithm. All Steiner points are inserted by splitting the edges.

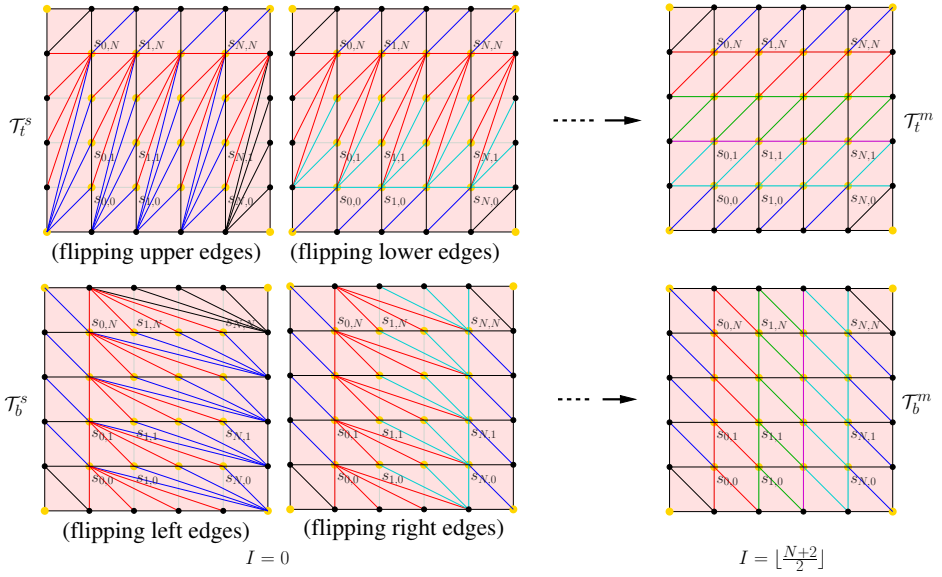

Fig. 9. An example result of the second step of the transformation algorithm. Two sequences of edge flips are applied on top and bottom triangulations, respectively. The resulting two triangulations $\mathcal{T}_t^m$ and $\mathcal{T}_b^m$ are shown on the right.

4.4. Proof of Correctness

In this section, we will show that the transformation algorithm does give a tetrahedralisation of the modified reduced Chazelle polyhedron $\Phi_{N,\varepsilon}^s$.

Consider the case when two planar triangles *abc* and *abd* are split by a point *p* that lies in the interior of the edge *ab*. It results four triangles, *apc*, *bpc*, *apd*, and *bpd*. Now placing the two original triangles *abc* and *bad* in $\mathbb{R}^3$, and

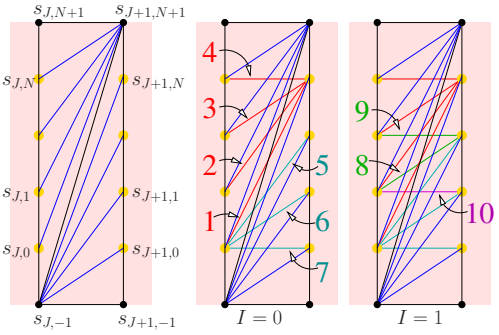

Fig. 10. An example of the sequence of edge flips applied on one section of the top triangulations $\mathcal{T}_t^s$. Left is the initial triangulation before the edge flips. Right shows the sequence is the newly created edges with their indices by the flip sequence.

shift the point p slightly away from the edge ab, and let the projection of them in the plane still remains the same picture. What we have in $\mathbb{R}^3$ are two tetrahedra $abpc$ and $abpd$. If we look from the top of them we see the two faces: abc and abd, and from bottom we see the other four faces all containing p. Hence a `split_edge` operation interchanges the two sets of outer faces of these two tetrahedra.

The `split_edge` operations in our algorithm (in the lines from 2 to 6) correspond to the removals of tetrahedra from $\Phi^s_{N,\varepsilon}$, and at the same time, the insertions of the Steiner points. This algorithm starts from the most outer boundary faces of $\Phi^s_{N,\varepsilon}$, for an example, the two faces $s_{J,-1}s_{J,N+1}s_{J-1,-1}$ and $s_{J,-1}s_{J,N+1}s_{J+1,N+1}$ sharing at the boundary edge $s_{J,-1}s_{J,N+1}$, and removes two tetrahedra $s_{J,-1}s_{J,N+1}s_{J-1,-1}s_{J,0}$ and $s_{J,-1}s_{J,N+1}s_{J+1,N+1}s_{J,0}$ from $\Phi^s_{N,\varepsilon}$. The removal of these two tetrahedra makes a "dent" in the outer boundary of $\Phi^s_{N,\varepsilon}$ which has now the four new triangles (the lower faces of the two removed tetrahedra) with the interior Steiner point $s_{J,0}$ on its boundary. The next `split_edge` operation continues to remove tetrahedra from the just exposed new boundary faces. For the same example as above, the two faces $s_{J,0}s_{J,N+1}s_{J-1,-1}$ and $s_{J,0}s_{J,N+1}s_{J+1,N+1}$ sharing at the boundary edge $s_{J,0}s_{J,N+1}$ are split, and the new interior Steiner points $s_{J,1}$ is inserted on the boundary. This process ends after all interior Steiner points are on the boundary $\Phi^s_{N,\varepsilon}$, as viewed in Figure 8. Note that the tetrahedra removed from top and bottom triangulations will not overlap, since they are separated by the saddle surface $z = xy + \omega$.

Now we turn to the second step of our algorithm, which uses the `flip_edge` operations to transform the top and bottom triangulations. We already showed that each `flip_edge` operation corresponds to a tetrahedron. We still need to show that this tetrahedron is valid, i.e., the removal of it does decrease the volume of $\Phi^s_{N,\varepsilon}$.

In $\mathcal{T}_t^b$, all the edges between the two line segments $s_{J,-1}s_{J,N+1}$ and $s_{J+1,-1}s_{J+1,N+1}$ are divided into two groups by the diagonal line segment $s_{J,-1}s_{J+1,N+1}$, where $J = -1, \ldots, N$. They are called *upper* and *lower* edges, respectively, see an example in Figure 10. Similarly, all edges in $\mathcal{T}_b^s$ between the two line segments $s_{-1,J}s_{N+1,J}$ and $s_{-1,J+1}s_{N+1,J+1}$ are divided into two groups by the diagonal line segment $s_{-1,J}s_{N+1,J-1}$, where $J = -1, \ldots, N$. They are called *left* and *right* edges, respectively.

Our transform algorithm will automatically generate two sequences of edge flips, i.e., the pseudocode from lines 8 to 21 in Figure 7, one in the top $\mathcal{T}_t^s$ and one in the bottom $\mathcal{T}_b^s$ triangulations. Each flip sequence is also divided into two subsequences, which are the flips to create the upper and lower edges in $\mathcal{T}_t^s$ and the flips to create left and right edges in $\mathcal{T}_b^s$. The order of these flip sequences ensures that the edges needed for the next flip exist. Figure 10 gives an example of all edges generated between one pair of line segments and the order of the edge flip sequence.

Now it remains to show that every edge flip in our algorithm will create a valid tetrahedron for $\Phi^s_{N,\varepsilon}$. In particular, there are four `flip_edge` operations (in line 12 and line 18 in Figure 7) in our algorithm, see Figure 11. They are used in the four subsequences of edge flips, respectively. Since each edge flip operation is a local operation, it is sufficient to show that each edge flip will create an interior edge of $\Phi^s_{N,\varepsilon}$. Hence the newly created edge together with the old edge form an interior tetrahedron of $\Phi^s_{N,\varepsilon}$. For this purpose, the following lemma is needed.

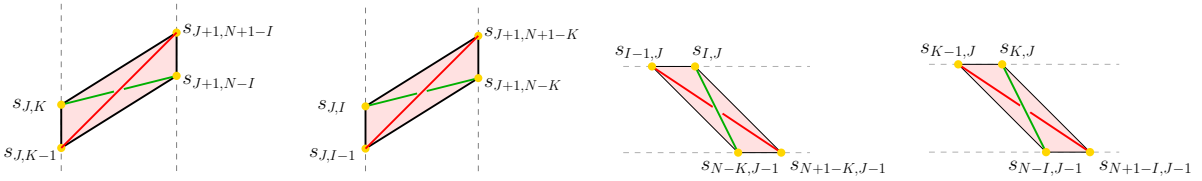

(1) in $\mathcal{T}_t^s$ upper (2) in $\mathcal{T}_t^s$ lower (3) in $\mathcal{T}_b^s$ left (4) in $\mathcal{T}_b^s$ right

Fig. 11. The four types of edge flips in the algorithm. In these figures, red edges are the input edges, green edges are the resulting edges. Each pair of red and green edges forms a tetrahedron in the interior of $\Phi^s_{N,\varepsilon}$.

Lemma 1. *Let $det(s_1, s_2, s_3, s_4)$ denote the determinant of the four points $s_1, \ldots, s_4 \in \mathbb{R}^3$. Then the following determinants on the set of Steiner points are all constant.*

$$\begin{aligned} &det(s_{J+1,N+1-I}, s_{J,K-1}, s_{J+1,N-I}, s_{J,K}) \equiv 1 \\ &det(s_{J,I-1}, s_{J+1,N+1-K}, s_{J,I}, s_{J+1,N-K}) \equiv 1 \\ &det(s_{I-1,J}, s_{N+1-K,J-1}, s_{I,J}, s_{N-K,J-1}) \equiv -1 \\ &det(s_{N+1-I,J-1}, s_{K-1,J}, s_{N-I,J-1}, s_{K,J}) \equiv -1 \end{aligned} \tag{1}$$

The above equalities can be proven by direct calculations (given in the Appendix).

This lemma ensures that each `flip_edge` operation in our algorithm will indeed create a valid tetrahedron in $\Phi^s_{N,\epsilon}$. In particular, Equation (1) indicates that the

$$\texttt{flip\_edge}(s_{J+1,N+1-I}, s_{J,K-1}, s_{J+1,N-I}, s_{J,K})$$

operation in the top triangulation $\mathcal{T}_t^s$ will create a new edge $s_{J+1,N-I}s_{J,K}$ that lies below the old edge $s_{J+1,N+1-I}s_{J,K-1}$, see Figure 11 (1). And the Equation (1) indicates that the

$$\texttt{flip\_edge}(s_{I-1,J}, s_{N+1-K,J-1}, s_{I,J}, s_{N-K,J-1})$$

operation in the bottom triangulation $\mathcal{T}_b^s$ will create a new edge $s_{I,J}s_{N-K,J-1}$ that lies above the old edge $s_{I-1,J}s_{N+1-K,J-1}$, see Figure 11 (3). The same are true for the other two `flip_edge` operations.

By this lemma, all tetrahedra corresponding to our edge flip sequences are valid. Another surprising fact is that the volumes of these tetrahedra are all equal and are independent of the parameters N, ε, and ω.

We thus can prove the following theorem:

Theorem 2. *There exists a tetrahedralisation of $\Phi^s_{N,\varepsilon}$ with the set $\mathcal{S}$ of interior Steiner points.*

Proof. Given a $\Phi^s_{N,\varepsilon}$, we apply the transformation algorithm in Figure 7 from its top and bottom triangulations to reduce the volume of $\Phi^s_{N,\varepsilon}$ by removing tetrahedra from $\Phi^s_{N,\varepsilon}$ corresponding to the `split_edge` and `flip_edge` operations. This will reduce $\Phi^s_{N,\varepsilon}$ into a 3d polyhedron P which has the two triangulations $\mathcal{T}_t^m$ and $\mathcal{T}_b^m$ (shown in Figure 9 right) as its boundary. It is easy to see that the set of tetrahedra

$$\mathcal{T}_m := \{s_{I-1,J-1}s_{I,J-1}s_{I-1,J}, s_{I,J} \mid I, J = 1, \ldots, N+1\}.$$

tetrahedralises P. □

5. Discussions

In this paper, we studied the problem of tetrahedralising reduced Chazelle polyhedra with interior Steiner points. We proposed a placement of Steiner points and show the existence of a tetrahedralisation with these Steiner points. In practice, the questions like "where to place Steiner points" and "How many of them are necessary?" are very important to know in order to design correct and efficient algorithms. Our result gives at least some suggestion on where the Steiner points could be placed. However, the optimal number of Steiner points remains an open question.

The set $\mathcal{S}$ of interior Steiner points is independent of the thickness ε of $\Phi^s_{N,\varepsilon}$. Here the thickness ε plays an important role in the needed number of interior Steiner points.

- There are $(N+1)^2$ Steiner points in $\mathcal{S}$ and it is indeed necessary to have all of them when the thickness ε is sufficiently small.
- If the thickness ε becomes larger, it is not necessary to use the full set of $(N+1)^2$ Steiner points. In particular, there must exist a bound on ε such that the reduced Chazelle polyhedron $\Phi^s_{N,\varepsilon}$ needs only a linear number of Steiner points.
- If the ε is large enough, the reduced Chazelle polyhedron becomes directly tetrahedralisable, i.e., no Steiner point is needed. There must exist such a bound on ε.

It is an interesting question to find the relation between ε and the number of Steiner points. This may be a interesting theoretical question for our future work.

Finally, there are indeed many possibilities to generalise the Chazelle polyhedron. One of such examples is found in [7]. More generally, it is possible to use any doubly-ruled surfaces instead of the saddle surfaces as the basic geometry structure.

References

[1] F. Bagemihl. On indecomposable polyhedra. *The American Mathematical Monthly*, 55(7):411–413, 1948.

[2] M. Bern. Compatible tetrahedralizations. In *Proc. 9th Annual ACM Symposium on Computational Geometry*, pages 281–288, 1993.

[3] Marshall W. Bern and David Eppstein. Mesh generation and optimal triangulation. In Ding-Zhu Du and Frank Kwang-Ming Hwang, editors, *Computing in Euclidean Geometry*, number 4 in Lecture Notes Series on Computing, pages 47–123. World Scientific, second edition, 1995.

[4] Bernard Chazelle. Convex partition of polyhedra: a lower bound and worst-case optimal algorithm. *SIAM Journal on Computing*, 13(3):488–507, 1984.

[5] Bernard Chazelle and Leonidas Palios. Triangulating a non-convex polytope. *Discrete & Computational Geometry*, 5(3):505–526, 1990.

[6] Mark de Berg and Chris Gray. Decompositions and boundary coverings of non-convex fat polyhedra. *Computational Geometry*, 43(2):73 – 83, 2010. Special Issue on the 24th European Workshop on Computational Geometry (EuroCG'08).

[7] Jeff Erickson. Local polyhedra and geometric graphs. *Computational Geometry*, 31(1-2):101–125, 2005.

[8] Paul-Louis George, Houman Borouchaki, and Eric Saltel. "Ultimate" robustness in meshing an arbitrary polyhedron. *International Journal for Numerical Methods in Engineering*, 58:1061–1089, 2003.

[9] Paul-Louis George, Frédéric Hecht, and Eric Saltel. Automatic mesh generator with specified boundary. *Computer Methods in Applied Mechanics and Engineering*, 92:269–288, 1991.

[10] Nadja Goerigk and Hang Si. On indecomposable polyhedra and the number of interior Steiner points. WIAS Preprint No. 2142, June 2015.

[11] J. Goodman and J. Pach. Cell decomposition of polytopes by bending. *Israel J. Mathematics*, 64:129–138, 1988.

[12] B. Kaan Karamete, Mark W. Beall, and Mark S. Shephard. Triangulation of arbitrary polyhedra to support automatic mesh generators. *International Journal for Numerical Methods in Engineering*, 49(12):167–191, 2000.

[13] Charles L. Lawson. Transforming triangulations. *Discrete Mathematics*, 3(4):365–372, 1972.

[14] Michael S. Paterson and F. Frances Yao. Efficient binary space partitions for hidden-surface removal and solid modeling. *Discrete & Computational Geometry*, 5(1):485–503, 1990.

[15] Jörg Rambau. On a generalization of Schönhardt's polyhedron. In J. E. Goodman, J. Pach, and E. Welzl, editors, *Combinatorial and Computational Geometry*, volume 52, pages 501–516. MSRI publications, 2005.

[16] Jim Ruppert and Raimund Seidel. On the difficulty of triangulating three-dimensional nonconvex polyhedra. *Discrete & Computational Geometry*, 7:227–253, 1992.

[17] E. Schönhardt. Über die Zerlegung von Dreieckspolyedern in Tetraeder. *Mathematische Annalen*, 98:309–312, 1928.

[18] Jonathan R. Shewchuk. Constrained Delaunay tetrahedralizations and provably good boundary recovery. In *Proc. 11th International Meshing Roundtable*, pages 193–204. Sandia National Laboratories, 2002.

[19] Jonathan R. Shewchuk. General-dimensional constrained Delaunay and constrained regular triangulations, I: combinatorial properties. *Discrete & Computational Geometry*, 39:580–637, 2008.

[20] Hang Si. TetGen, a Delaunay-based quality tetrahedral mesh generator. *ACM Trans. Math. Softw.*, 41(2):11:1–11:36, February 2015.

[21] Hang Si and Klaus Gärtner. 3D boundary recovery by constrained Delaunay tetrahedralization. *International Journal for Numerical Methods in Engineering*, 85:1341–1364, 2011.

[22] Hang Si and Jonathan R. Shewchuk. Incrementally constructing and updating constrained Delaunay tetrahedralizations with finite precision coordinates. In *Proceedings of the 21th International Meshing Rountable*, pages 173–190. Sandia National Laboratories, 2012.

[23] Daniel D. Sleator, William P. Thurston, and Robert Endre Tarjan. Rotation distance, triangulations, and hyperbolic geometry. *J. Amer. Math. Soc.*, 1:647–682, 1988.

[24] TetMesh-GHS3D. a powerful isotropic tet-mesher, 2012.

[25] G. T. Toussaint, C. Verbrugge, C. Wang, and B. Zhu. Tetrahedralization of simple and non-simple polyhedra. In *Proc. 5th Canadian Conference on Computational Geometry*, pages 24–29, 1993.

[26] Nigel P. Weatherill and Oubay Hassan. Efficient three-dimensional Delaunay triangulation with automatic point creation and imposed boundary constraints. *International Journal for Numerical Methods in Engineering*, 37:2005–2039, 1994.